Dehydrochlorination of Intermediates in the Production of Vinyl Chloride over Lanthanum Oxide-Based Catalysts

ARTICLE *in* CATALYSIS LETTERS · APRIL 2008

Impact Factor: 2.31 · DOI: 10.1007/s10562-008-9436-2

4 AUTHORS, INCLUDING:

René Bogerd

3 PUBLICATIONS **49** CITATIONS

SEE PROFILE

Bert M Weckhuysen

Utrecht University

594 PUBLICATIONS **16,702** CITATIONS

SEE PROFILE

Catal Lett (2008) 122:238–246
DOI 10.1007/s10562-008-9436-2

Dehydrochlorination of Intermediates in the Production of Vinyl Chloride over Lanthanum Oxide-Based Catalysts

Alwies W. A. M. van der Heijden · Ad J. M. Mens · René Bogerd · Bert M. Weckhuysen

Received: 15 December 2007 / Accepted: 8 February 2008 / Published online: 28 March 2008

Abstract Lanthanum oxide-based catalysts are active in the elimination of HCl from C_2H_5Cl, 1,2-$C_2H_4Cl_2$ and 1,1,2-$C_2H_3Cl_3$ leading to the formation of their respective chlorinated ethenes. An oxygen-rich catalytic surface may form CO, CO_2 and C_2HCl as side products, whereas with chlorine-rich catalytic surfaces a stable product distribution is achieved with 100% selectivity towards the formation of ethenes, such as the valuable C_2H_3Cl intermediate.

Keywords Dehydrochlorination · Heterogeneous catalysis · Lanthanum oxide · Chlorinated ethanes · Gas phase IR

1 Introduction

With an annual production of 45 million tons, chlorine is one of the most important chemicals for numerous commercial products [1]. The reaction with chlorine activates hydrocarbons, making them suitable as building blocks for organic synthesis. Moreover, chlorinated hydrocarbons (CHCs) are used as organic solvents and are persistent, making them heat-resistant and relatively inert. On the other hand, the same properties which make these compounds useful in industry make them harmful when emitted into the environment. In the last decades, it was found that CHCs contribute to various environmental effects, such as acid rain formation, ozone layer depletion and the greenhouse effect [2–4]. Also, many CHCs are carcinogenic and toxic. Even though the better understanding of the effects of these substances has greatly reduced the use in commercial applications, they are still used and produced in large quantities in industry [5].

More than one third of all chlorine is used for the production of polyvinyl chloride (PVC), the most produced plastic in the world after polyethylene (PE) [1, 5]. C_2H_3Cl is the monomer of PVC and is industrially prepared from C_2H_4 and chlorine. C_2H_4 is chlorinated into 1,2-$C_2H_4Cl_2$ via oxychlorination and direct chlorination described by Reaction Equations (1) and (2), respectively. 1,2-$C_2H_4Cl_2$ is then thermally cracked into C_2H_3Cl as shown in Reaction Equation (3). The oxychlorination process is used to lower chlorine consumption by recycling HCl from the cracking of 1,2-$C_2H_4Cl_2$, though selectivity towards 1,2-$C_2H_4Cl_2$ is lower than for the direct chlorination process. Overall, the reactions are performed at relatively high selectivity (>98%), but the scale of the process result in the formation of large quantities of by-products [6]. Various chlorinated C_1 and C_2 are formed in side- reactions and are separated from 1,2-$C_2H_4Cl_2$ as the so-called light and heavy ends. Regulation on the production and emission [2–4] of CHCs has enforced efficient degradation of excess CHCs, which is done in most cases by incineration [7]. However, because of the high heat resistance of the CHCs and possible formation of furans and dioxins, a high temperature (>1,000 °C) is needed for this process, making it costly. In addition, incineration results in loss of feedstock.

$$C_2H_4 + {}^1/_2\,O_2 + 2\,HCl \rightarrow 1,2\text{-}C_2H_4Cl_2 + H_2O \quad (1)$$

$$C_2H_4 + Cl_2 \rightarrow 1,2\text{-}C_2H_4Cl_2 \quad (2)$$

$$1,2\text{-}C_2H_4Cl_2 \rightarrow C_2H_3Cl + HCl \quad (3)$$

Research efforts have been made on methods to efficiently convert CHCs at low temperature into non-hazardous or

A. W. A. M. van der Heijden · A. J. M. Mens · R. Bogerd · B. M. Weckhuysen (✉)
Inorganic Chemistry and Catalysis Group, Department of Chemistry, Faculty of Science, Utrecht University, Sorbonnelaan 16, 3584 CA Utrecht, The Netherlands
e-mail: b.m.weckhuysen@uu.nl

re-usable products. Catalytic (hydro)dechlorination can be categorized by three types of systems: noble metals, transition metal oxides and basic oxides. In the case of noble metals, poisoning of the catalyst by chlorine remains a difficult issue to overcome [8–13]. Even though transition metal oxides are very active for the dechlorination of CHCs, the chlorination of the oxide may result in the formation of toxic volatile transition metal oxychlorides [14–21]. The basic oxides have proven to be stable active materials for the conversion of CHCs [22–34]. In previous work, lanthanum oxide-based catalysts were found to have the highest destructive capacity for the catalytic destruction of chlorinated C_1 and have been studied in detail in our group [29–31, 33, 34]. However, activity towards both chlorinated C_1 and C_2 is important for conversion of the light ends mixture formed in C_2H_3Cl production.

1,1-$C_2H_2Cl_2$, which is the monomer for the production of polyvinylidene chloride (PVDC), is prepared from the dehydrochlorination of 1,1,2-$C_2H_3Cl_3$ using alkaline solutions [35]. Actually, in most cases 1,1,2-$C_2H_3Cl_3$ is used to produce 1,1-$C_2H_2Cl_2$, since sufficient quantities are formed during the production of C_2H_3Cl. Also, the cracking of 1,2-$C_2H_4Cl_2$ to C_2H_3Cl is a non-catalytic dehydrochlorination reaction. Not many heterogeneous catalysts are known for the dehydrochlorination of chlorinated ethanes, mainly because of low selectivity and chlorine poisoning. In fact, alumina is active for this reaction and has been studied because dehydrochlorination is an undesirable side-reaction in the oxychlorination of ethene into 1,2-$C_2H_4Cl_2$, which is catalyzed by $CuCl_2/\gamma$-Al_2O_3 [36, 37]. Therefore, catalytic dehydrochlorination of chlorinated ethanes is not only interesting from a waste conversion point of view as an active dehydrochlorination catalyst could be used in the preparation steps towards C_2H_3Cl as well. Here, we report for the first time on such new active dehydrochlorination catalyst based on lanthanum oxides, which leads to the selective formation of C_2H_3Cl when starting from 1,2-$C_2H_4Cl_2$.

2 Experimental

2.1 Materials and Characterization

Commercial samples of La_2O_3 (Acros Organics, 99.99%) were used without additional purification. LaOCl was synthesized by a precipitation process using $LaCl_3.7H_2O$ (Acros Organics, 99.99%) as precursor and a NH_4OH (Merck, 25 wt% in water p.a.) solution. The obtained gel ($La(OH)_2Cl$) was filtered, washed and dried at 120 °C and heated at 550 °C in pure N_2 (Linde, ≥99.999%) for 6 h. The phase composition of La_2O_3 and LaOCl after the reaction as a function of time with 1,1,2-$C_2H_3Cl_3$ was determined using X-ray diffraction (XRD) and X-ray photoelectron spectroscopy (XPS). XRD measurements were performed at ambient conditions with a Bruker-AXS D8 diffractometer equipped with a $Co_{K\alpha 1,2}$ source. The XPS spectra were acquired using a Perkin-Elmer (PHI) model 5500 spectrometer. All XPS spectra were obtained using samples in the form of pressed wafers.

2.2 Flow Gas Experiments

The activity experiments for the dehydrochlorination of C_2H_5Cl (Aldrich, ≥99.7%), 1,2-$C_2H_4Cl_2$ (Acros Organics, ≥99.8%) and 1,1,2-$C_2H_3Cl_3$ (Acros Organics, ≥98%) were performed in a tubular fixed-bed quartz reactor. The catalyst bed consisted of 0.5 g LaOCl or La_2O_3 pressed in a 200–500 μm sieve fraction, pretreated in 10 mL/min He (Linde, ≥99.996%) at 550 °C. The flow was regulated by Brooks 0–100 mL automatic mass flow controllers. To find the initial reaction temperature, the reaction was carried out from 50 to 400 °C using a 25 mL/min 3–4 vol% reactant/He flow. In the case of 1,2-$C_2H_4Cl_2$ and 1,1,2-$C_2H_3Cl_3$, the flow was generated by flowing He through a bubbler containing the liquid reactant. The C_2H_5Cl feed was generated from 2 mL/min C_2H_5Cl and 23 mL/min He. Once stabilized, the flow was led over the reactor bed, consisting of LaOCl or La_2O_3. The temperature of the reactor was raised from 50 to 400 °C in steps of 10 °C. The heating ramp was 3.3 °C/min, and after each step, the temperature was held constant for 5 min. The composition of the reactor effluent was analyzed by a Siemens Maxum Edition 2 gas chromatograph with a sampling time of 240 s. In the case of 1,1,2-$C_2H_3Cl_3$, the reactions were also performed at constant temperature of 400 °C over La_2O_3 and LaOCl. The composition of the reaction mixture was analyzed with time.

2.3 IR Experiments

During the flow gas experiments with 1,1,2-trichloethane over La_2O_3, several products were detected which could not be assigned by GC. To complement the GC data, the reaction of 1,1,2-trichloethane on La_2O_3 was monitored in situ by IR. A static vacuum quartz cell was employed and all IR spectra were recorded using a Perkin Elmer 2000 spectrometer with a resolution of 4 cm^{-1}. La_2O_3 (Acros Organics, 99.99%) was pressed into a self-supporting wafer (2 cm^2), and activated in situ prior to the IR measurements in dynamic vacuum at 550 °C overnight. 1,1,2-$C_2H_3Cl_3$ (Acros Organics, 98%) was evaporated by injection via a septum into an evacuated flask, which was connected to the vacuum system. After pretreatment, 1,1,2-$C_2H_3Cl_3$ (30 mbar) was introduced into the cell, which was then closed. The wafer was positioned in a separate heated part

of the cell, enabling the measurement of gas phase IR spectra. The temperature was raised from 100 to 400 °C in steps of 50 °C. After each step the temperature was held constant during which gas phase spectra were recorded.

3 Results and Discussion

3.1 Temperature Programmed Reaction Studies on the Catalyst Activity and Selectivity

The effluent composition of the temperature programmed dehydrochlorination reactions over LaOCl is shown in Fig. 1. In the case of C_2H_5Cl and 1,2-$C_2H_4Cl_2$, 100% selectivity is observed towards C_2H_4 and C_2H_3Cl, respectively (Reaction Equations (4) and (5)). 1,1,2-$C_2H_3Cl_3$ is converted into several products. A significantly lower initial reaction temperature is observed for chloroethane compared to 1,2-$C_2H_4Cl_2$ and 1,1,2-$C_2H_3Cl_3$. It has been established that the cleavage of the C–Cl bond typically precedes the removal of a H atom [38, 39]. Furthermore, it has been shown that the initial reaction rate for the dehydrochlorination of chlorinated ethanes increases with an increasing number of chlorine atoms [40]. It should be noted, however, that this trend was established based on mono-, di- and tri-substituted chloroethanes with all chlorine atoms on the same carbon atom. With more C–Cl bonds on the same carbon atom in a chlorinated ethane molecule, the C–Cl bonds become more polarized. As a result, the C–Cl bonds are more susceptible to cleavage. Instead, C–Cl bonds on both carbon atoms may stabilize the polarization of the C–Cl bonds, which explains the higher initial temperature of reaction of 1,2-$C_2H_4Cl_2$ and 1,1,2-$C_2H_3Cl_3$ with respect to C_2H_5Cl.

The main product for the dehydrochlorination of 1,1,2-$C_2H_3Cl_3$ is 1,1-$C_2H_2Cl_2$ and in addition C_2H_3Cl and cis-1,2-$C_2H_2Cl_2$ are formed. The formation of C_2H_3Cl implies that Cl_2 elimination occurs. This reaction is, however, energetically highly unfavourable and is not expected to proceed. A possible explanation would be that a different product is co-eluting with C_2H_3Cl. Therefore, the product assigned by the GC as C_2H_3Cl has been labelled as X in Figs. 1 and 2. Chlorine and hydrogen atoms can be removed from the reactant molecule via two pathways of HCl elimination, shown in Reaction Scheme 1. The formation of 1,1-$C_2H_2Cl_2$ (Scheme 1, Reaction a) is favoured over the reaction towards 1,2-$C_2H_2Cl_2$ (Scheme 1, Reaction b). In addition, no formation of trans-1,2-$C_2H_2Cl_2$ (Scheme 1, Reaction c) was detected. At 400 °C, trace amounts of CO and CO_2 were detected. Blank experiments were also performed and no significant product formation was observed, which rules out non-catalytic gas phase reactions. Based on these results, it is concluded that LaOCl is an active catalyst for the dehydrochlorination of chlorinated ethanes.

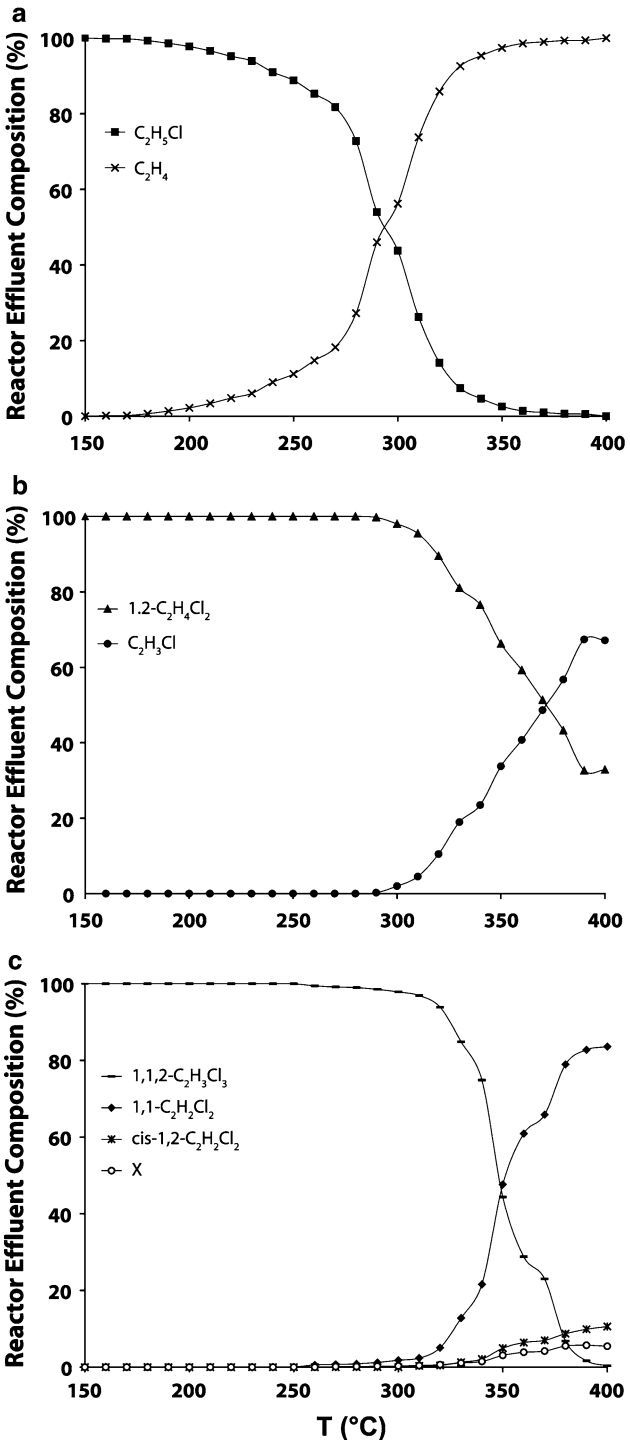

Fig. 1 Effluent composition for the dehydrochlorination of (**a**) C_2H_5Cl, (**b**) 1,2-$C_2H_4Cl_2$ and (**c**) 1,1,2- $C_2H_3Cl_3$ over LaOCl as a function of temperature. (GHSV = 2,000 h^{-1}, inlet concentration: [C_2H_5Cl] = 3.7 vol%, [1,2-$C_2H_4Cl_2$] = 3.4 vol% and [1,1,2-$C_2H_3Cl_3$] = 3.2 vol%, X = product unassigned based on GC)

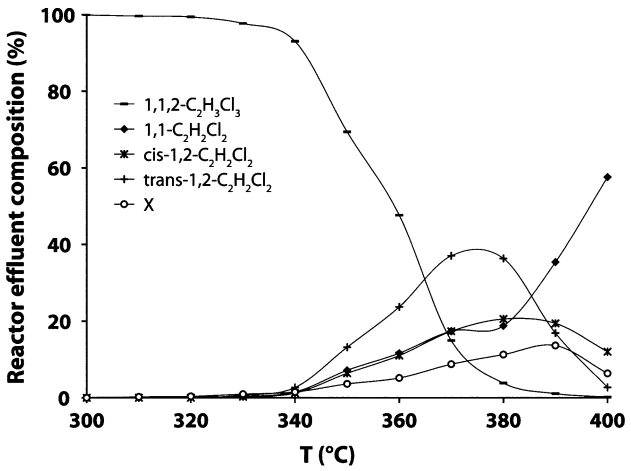

Fig. 2 Effluent composition for the dehydrochlorination of 1,1,2-$C_2H_3Cl_3$ over La_2O_3 as a function of temperature. (GHSV = 2,000 h^{-1}, inlet concentration: [1,1,2-$C_2H_3Cl_3$] = 3.2 vol%, X = product unassigned based on GC)

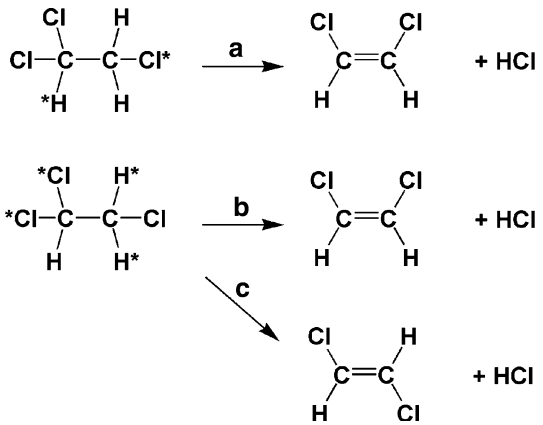

Scheme 1 Reaction pathways for the dehydrochlorination of 1,1,2-$C_2H_3Cl_3$ into (**a**) 1,1-$C_2H_2Cl_2$, (**b**) cis-1,2-$C_2H_2Cl_2$ and (**c**) trans-1,2-$C_2H_2Cl_2$

$$CH_2Cl\text{-}CH_3 \rightarrow CH_2 = CH_2 + HCl \quad (4)$$

$$CH_2Cl\text{-}CH_2Cl \rightarrow CH_2 = CHCl + HCl \quad (5)$$

The dehydrochlorination of chlorinated ethanes over heterogeneous catalysts is catalyzed by three types of active sites: acidic, basic or dual sites [41]. It has been shown that for the dehydrochlorination of 1,1,2-trichloroethane, the selectivity towards the 1,1- and 1,2-product are influenced by the acid-base properties of the catalyst [41]. Control of the chlorination degree of the catalyst is crucial to tune the acid-base properties and optimize the performance of the catalyst when converting mixtures of chlorinated C_1 and C_2. In previous work, it was shown that the acid-base properties of lanthanum oxide-based catalysts are a key factor for the activation of C–Cl and C–H bonds in chlorinated C_1 [33, 34]. Hence, the degree of chlorination may also be of influence on the selectivity of the dehydrochlorination of chlorinated C_2. Therefore, the reaction with 1,1,2-$C_2H_3Cl_3$ was repeated with La_2O_3, which contains weaker La^{3+} Lewis acid sites. The reactor effluent composition was analyzed throughout the experiment, as shown in Fig. 2. In addition to the products observed over LaOCl, trans-1,2-$C_2H_2Cl_2$ is detected. However, as the temperature increases the selectivity towards 1,1-$C_2H_2Cl_2$ increases, while it decreases towards the other products. Low concentrations of CO and CO_2 were detected as in the case of LaOCl. Also, small amounts of two products were detected which could not be assigned based on the GC results. Even though these products could not be identified, the retention times indicate that these compounds are CHCs. Therefore, the same response factor as for the other CHCs is assumed to be valid for these unknown products.

3.2 In Situ IR Studies on the Catalyst Activity and Selectivity

The flow-gas experiments indicate that La_2O_3 and LaOCl catalyze the dehydrochlorination of chlorinated ethanes and that the acid-base properties of the catalyst directly influence the selectivity. However, the assignment of the products is difficult with gas chromatography only. Therefore, the gas phase composition of the temperature programmed reaction on La_2O_3 in a vacuum cell was monitored using IR spectroscopy to complement the GC results. The recorded spectra are shown in Fig. 3. In the spectral regions 2,250–2,400 and 1,350–1,900 cm^{-1}, the strong bands of ambient CO_2 and H_2O, respectively, were removed by spectroscopic software. Figure 3a illustrates the increase and decrease of the bands in the gas phase spectra as a function of temperature during the experiment. In Fig. 3b, the spectrum of the reactant at room temperature (RT) is shown together with that of Spectrum 11 from Fig. 3a. Spectrum 11 was chosen for the assignment of the bands of the products, because all the bands which are observed during the experiment are present in this spectrum.

The assignment of the bands based on reference spectra is shown in Table 1 [42]. The products that are formed throughout the experiment are 1,1-$C_2H_2Cl_2$, cis-1,2-$C_2H_2Cl_2$, trans-1,2-$C_2H_2Cl_2$, C_2HCl, CO and CO_2. Specific bands were chosen, which possesses high intensity and minimal overlap with other bands, to derive the relative ratios of the products as a function of temperature as shown in Fig. 3a. The spectra show that $C_2H_2Cl_2$ derivatives are formed simultaneously at 200 °C (Fig. 3a, spectrum 4).

As the temperature increases (Fig. 3a, spectrum 5–9), the intensity of the chlorinated ethene bands increases with maximum intensity at 250 °C (Fig. 3a, spectrum 9). Further increase of the temperature results in a decrease in intensity

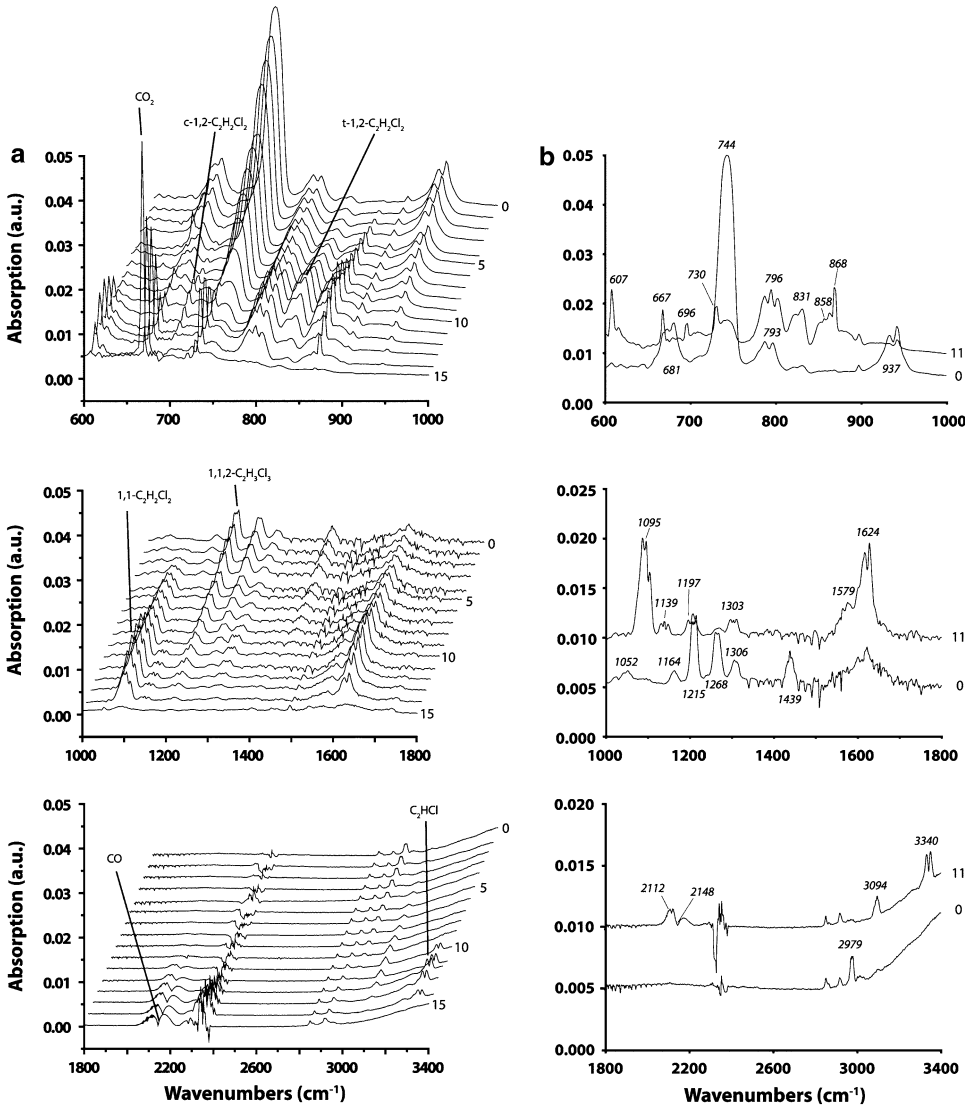

Fig. 3 (**a**) Gas phase IR spectra recorded during the dehydrochlorination of 1,1,2-$C_2H_3Cl_3$ over La_2O_3 as a function of temperature: (0) reactant at RT, (1) 5 min at 100 °C, (2) 5 min at 150 °C, (3) 5 min at 200 °C, (4–6) 5, 10 and 25 min at 250 °C, (7–9) 5, 10 and 25 min at 300 °C, (10–12) 5, 10 and 25 min at 350 °C, (13–15) 5, 10 and 75 min at 400 °C. (**b**) Spectrum (0) and (11) used for band assignment of products

of the bands assigned to cis/trans-1,2-$C_2H_2Cl_2$. The intensity of the 1,1-$C_2H_2Cl_2$ band, however, remains constant. The decrease in intensity of the bands of the 1,2-derivatives is accompanied by the formation of CO, CO_2 and C_2HCl (Fig. 3a, spectrum 10). The formation of C_2HCl indicates that a second dehydrochlorination reaction may occur resulting in the formation of a C ≡ C bond. At 350 °C, a band becomes visible at 730 cm^{-1}, for which a reference could not be found. Strong absorption at this position is characteristic for C–Cl stretch vibrations. When the temperature reaches 400 °C, the bands of C_2HCl and 1,1-$C_2H_2Cl_2$ also decrease and a strong increase in intensity of the CO_2 band is observed. The formation of CO and CO_2 is characteristic products for destructive adsorption of CHCs. After more than 1 h of reaction, only CO and CO_2 are detected. These results show that high temperatures should be avoided to prevent undesirable secondary reactions.

No bands indicative of C_2H_3Cl were observed in the spectra. The other products which were detected during the temperature programmed flow-gas experiment over La_2O_3 (Fig. 2), namely 1,1-$C_2H_2Cl_2$ and cis/trans-1,2-$C_2H_2Cl_2$, were also observed in the in situ IR experiment. Therefore, based on these spectra it is proposed that the product which co-elutes with C_2H_3Cl is C_2HCl. The dehydrochlorination of 1,1,2-$C_2H_3Cl_3$ proceeds at relatively low temperature. At higher temperature, two secondary reactions of the chlorinated ethenes are favorable; a second elimination of HCl or destructive adsorption. The former results in the formation of C_2HCl. The latter results in the breaking of the C–C bond and formation of CO and CO_2 via exchange of oxygen and chlorine atoms. The 1,2-$C_2H_2Cl_2$ derivatives are more susceptible to the secondary reactions than 1,1-$C_2H_2Cl_2$. It should be noted that no significant amounts of CO and CO_2 were detected during the flow-gas experiments. A possible reason

Table 1 Assignment of the gas phase IR bands in spectrum recorded after 10 min of conversion of 1,1,2-trichloethane over La_2O_3 at 350 °C shown in Fig. 3b. (vs = strong, s = strong)

Spectrum 11	1,1-$C_2H_2Cl_2$	c-1,2-$C_2H_2Cl_2$	t-1,2-$C_2H_2Cl_2$	C_2HCl	CO_2	CO
607	603 (s)					
667					667 (s)	
696		697 (vs)				
796	800 (vs)					
831			828 (vs)			
858		857 (vs)				
868	875 (vs)					
1095	1095 (vs)					
1139	1139 (s)					
1197			1200 (s)			
1303		1303 (s)				
1579		1574 (s)				
1624	1627 (vs)					
2112				2110 (s)		
2148						2144 (vs)
3094			3090 (s)			
3340				3340 (vs)		

for this may be the different nature of the experiments; the IR experiments are in a closed cell as opposed to the flow-gas experiment in which the reactant has a limited residence time.

3.3 Catalyst Behaviour

The temperature programmed flow-gas experiment over La_2O_3 suggests there is an induction period during which the selectivity changes. This is supported by the in situ IR experiments. Moreover, no bands indicative of HCl were found in the gas phase spectra. It is known that La_2O_3 and LaOCl can be chlorinated into a pure $LaCl_3$ phase using HCl. The HCl reacts with the basic oxygen sites according to Reaction Equation (6). During the dehydrochlorination of chlorinated ethanes, HCl may either be re-adsorbed or the H and Cl atom are abstracted directly by the La-O couple and remain on the surface. Either way, the catalytic surface will change which may affect the activity and selectivity. The stability of LaOCl and La_2O_3 materials for the dehydrochlorination of 1,1,2-$C_2H_3Cl_3$ was tested in a flow-gas experiment at 400 °C. The reactor effluent composition as a function of time is shown in Fig. 4. The experiment over La_2O_3 was stopped prematurely because the reactor became plugged. The experiments show that over La_2O_3, an induction period precedes a stable conversion and product distribution. The same products which were detected during the temperature programmed reactions are formed. The two unknown products, labelled x1 and x2, are formed at higher concentrations than during the temperature programmed experiments and are therefore included in Fig. 4. In the case of LaOCl, the induction period is not observed. After the induction period, the product distribution in the constant temperature experiments is similar for both LaOCl and La_2O_3. Although coke formation was observed, no significant loss of activity occurs in the experiments. LaOCl has proven to be a more stable catalyst with high selectivity towards chlorinated ethenes.

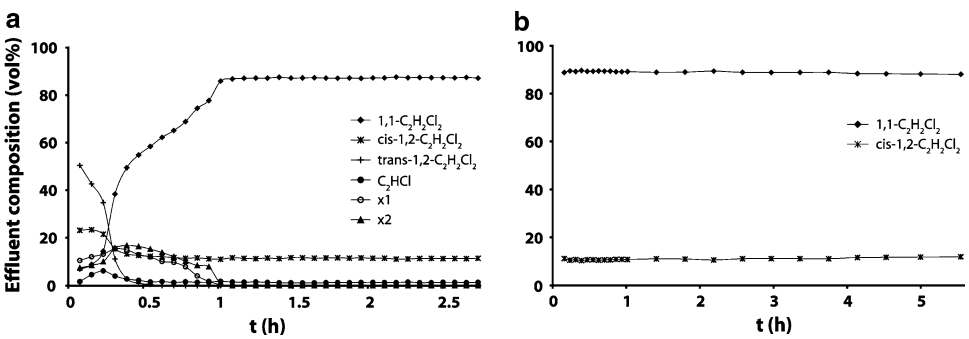

Fig. 4 Effluent composition for the dehydrochlorination of 1,1,2-$C_2H_3Cl_3$ over (**a**) La_2O_3 and (**b**) LaOCl at 400 °C as a function of time. (GHSV = 2,000 h^{-1}, inlet concentration: [1,1,2-$C_2H_3Cl_3$] = 3.2 vol%, x_n = product unassigned based on GC and IR)

$$\text{La-O-La (s)} + \text{HCl (g)} \rightarrow \text{La-OH (s)} + \text{Cl-La (s)} \quad (6)$$

Even though the GC is not calibrated for HCl and H_2O, these products are visible in the chromatogram at low retention times. The intensities of the peaks assigned to HCl and H_2O are shown in Fig. 5 as a function of time. The hydroxyl groups formed after HCl elimination can react into both HCl and H_2O. Initially, H_2O is eliminated from the oxygen-rich catalytic surface according to Reaction Equation (7). As the reaction proceeds, less hydroxyl groups are available and more chlorine is present on the surface. As a result, elimination of HCl from the surface becomes more favourable. The reaction time at which HCl formation becomes more dominant than H_2O formation, is also when the product distribution becomes stable. Therefore, it is proposed that a specific degree of chlorination of the catalyst material results in steady-state conversion of chlorinated ethanes. It should be noted that a small amount of H_2O is probably still formed together with HCl once the product distribution has stabilized, but due to overlap of the H_2O and HCl peak, the intensity of the H_2O peak is considered zero.

$$2\ \text{La-OH (s)} \rightarrow \text{H}_2\text{O (g)} + \text{La-O-La (s)} \quad (7)$$

If a specific chlorination degree is needed for steady-state conversion, the catalyst materials used in the constant temperature experiments should possess similar surface compositions. To verify this, the LaOCl and La_2O_3 catalyst were characterized before and after reaction with 1,1,2-trichloethane using XPS and XRD. The XRD results, as shown in Fig. 6, provide information on the bulk phase composition of the catalyst materials. Before reaction, the characteristic diffraction patterns of LaOCl and La_2O_3 are observed (Fig. 6a and c, respectively). The diffractogram of La_2O_3 after approximately 3 h of reaction at 400 °C is shown in Fig. 6b. The peaks observed after reaction show that during reaction the crystalline La_2O_3 phase has been converted into a pure crystalline LaOCl phase. Even though the peaks are much broader in the amorphous LaOCl catalyst material, the similarity is straightforward. The dehydrochlorination of 1,1,2-trichloethane at 400 °C over LaOCl was performed for ca. 6 h, which is over two

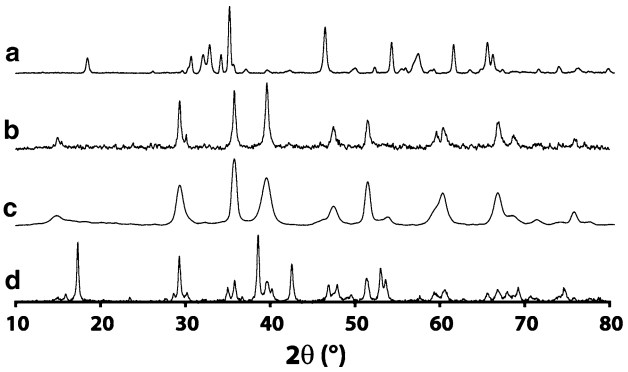

Fig. 6 X-ray diffractograms of La_2O_3 and LaOCl before (**a** and **c**, respectively) and after (**b** and **d**, respectively) the dehydrochlorination of 1,1,2-$C_2H_3Cl_3$ at 400 °C, as shown in Fig. 4

times as long as in the case of La_2O_3. The pattern of the LaOCl phase is partially preserved after reaction. However, a second phase is present, which was assigned as $LaCl_3 \cdot 3H_2O$. The peaks at $2\theta = 17.3$, 29.2, 38.5, 42.5 and 46.9 ° and their relative intensities are characteristic of $LaCl_3 \cdot 3H_2O$. It is uncertain whether LaOCl is converted into $LaCl_3 \cdot 3H_2O$ directly or into $LaCl_3$, which becomes hydrated when it is exposed to air prior to the XRD measurement. Either way, the bulk phase of both La_2O_3 and LaOCl has become chlorinated during the constant temperature reactions. Chlorination of the bulk phase is also observed during the destructive adsorption and catalytic destruction of chlorinated C_1 [29–33]. This is caused by the solid-state diffusion of oxygen and chlorine atoms between the catalytic surface and the bulk. As the surface becomes chlorinated, the chlorine atoms diffuse into the bulk and surface oxygen is regenerated. It is therefore viable to assume that the same process occurs when the surface becomes chlorinated as a result of the dehydrochlorination reaction.

The surface composition of LaOCl and La_2O_3 before and after reaction was determined with XPS. All spectra were normalized to the La3d band. Because lanthanum oxide-based materials strongly adsorb CO_2 and H_2O, the exposure to air may influence the characterization of O atoms. The intensity of the Cl2p band was therefore chosen

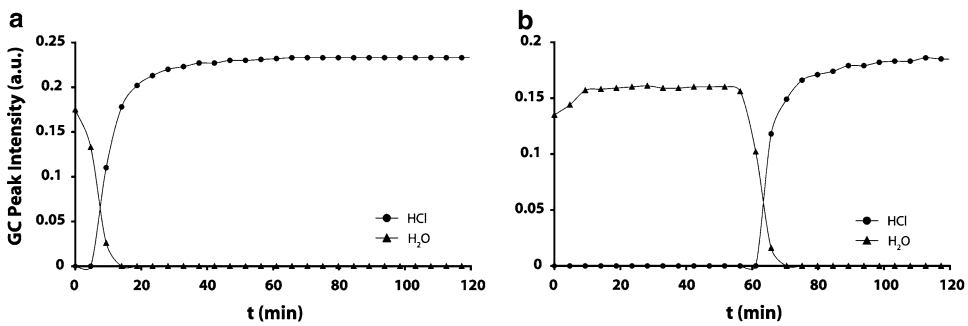

Fig. 5 Intensity of H_2O and HCl peak in the chromatograms of for the dehydrochlorination of 1,1,2-$C_2H_3Cl_3$ over (**a**) La_2O_3 and (**b**) LaOCl at 400 °C as a function of time as shown in Fig. 4. (GHSV = 2,000 h^{-1}, inlet concentration: [1,1,2-$C_2H_3Cl_3$] = 3.2 vol%, x_n = product unassigned based on GC and IR)

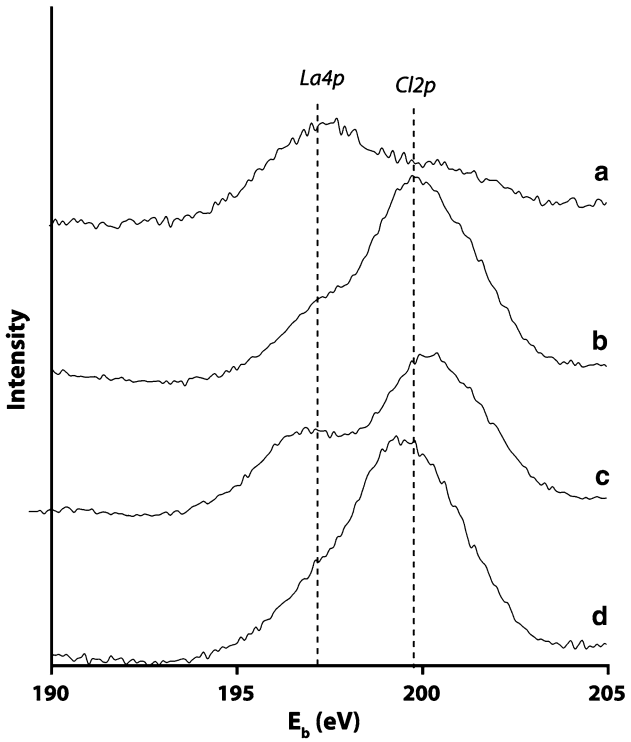

Fig. 7 X-ray photoelectron spectra of La_2O_3 and LaOCl before (**a** and **c**, respectively) and after (**b** and **d**, respectively) the dehydrochlorination of 1,1,2-$C_2H_3Cl_3$ at 400 °C, as shown in Fig. 4

as a measure of surface chlorination. Figure 7 shows the Cl2p band for LaOCl and La_2O_3 before and after reaction. The Cl2p band is obviously not observed in the spectrum of La_2O_3 before reaction (Fig. 7a). However, the La4p band is observed in the same region at 207 eV. Both these XPS bands are known to possess a shoulder at higher energy than the maximum, which is also observed here. The La4p band appears as a shoulder of the Cl2p band in the spectra of the materials containing chlorine. The Cl2p band positioned at 200 eV is observed in Fig. 7b–d. The spectra show that the surface chlorination of the materials after reaction is approximately the same and in both cases higher than before reaction. This result confirms the hypothesis that a specific degree of chlorination is required to reach steady-state conversion.

4 Conclusion

Lanthanum oxide-based materials are active catalysts for the dehydrochlorination of chlorinated ethanes. The reaction scheme for the dehydrochlorination of chlorinated ethanes over La_2O_3-based catalyst materials is schematically shown in Scheme 2. A hydrogen and chlorine atom is abstracted from the chlorinated ethane, resulting in the formation of a hydroxyl group and a lattice chloride (Scheme 2, Reaction b). In the case of an O-rich surface, such as La_2O_3, the hydroxyl groups will react with other hydroxyl groups under formation of H_2O (Scheme 2, Reaction c). However, when a specific degree of chlorination of the catalytic surface is reached, the elimination of H_2O becomes less pronounced and HCl is formed according to Reaction a in Scheme 2. After the induction period characterized by the formation of H_2O, the product distribution and conversion become stable and the chlorination degree of the catalyst surface also remains constant.

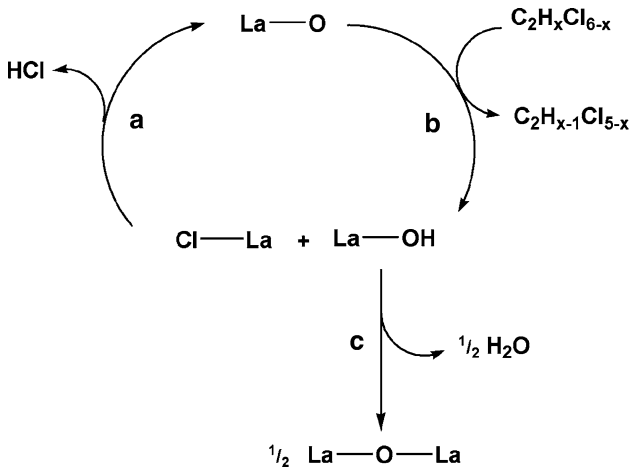

Scheme 2 Catalytic cycle for the dehydrochlorination of chlorinated ethanes over lanthanum oxide-based materials: (**a**) desorption of HCl from the catalyst material, (**b**) H + Cl abstraction by catalytic surface and (**c**) desorption of H2O from the catalyst material

The in situ IR experiments have shown that at relatively high temperature, secondary reactions may occur, such as a second dehydrochlorination step resulting in the formation of an ethyne, or destructive adsorption leading to the formation of CO and CO_2. This indicates that the reaction temperature and chlorination degree are key factors to achieve optimal selectivity towards the formation of ethenes. Because the chlorination degree of the catalyst is of influence on both activity and selectivity for the conversion of chlorinated C_1 and C_2, it may be used to tune the catalytic properties of the La_2O_3-based catalyst. This control of activity and selectivity is crucial for the efficient conversion of chlorinated waste streams, such as the light ends in the production of C_2H_3Cl.

Acknowledgments This work was supported by the National Research School Combination Catalysis (NRSCC) and an NWO-CW VICI Grant.

References

1. Bartsch R, Curlin CL, Florkiewicz TF, Lüke B, Minz H-R, Navin T, Scannell R, Schmittinger P, Zelfel E (2000) Chlorine: principles and industrial practice. Wiley-VCH, Weinheim
2. US Environmental Protection Agency (EPA) (1990) The clean air act of 1990, a primer on consensus building. Government Printing Office, Washington
3. Intergovernmental Panel on Climate Change (1990) In: Houghton JT, Jenkins GJ, Ephraums JJ (eds) Climate change: The IPCC scientific assessment. Cambridge University Press, Cambridge
4. Ozone Secretariat United Nations Environment Programme (2006) Handbook for the montreal protocol on substances that deplete the ozone layer 7th ed. Secretariat of the Vienna convention for the protection of the ozone layer and the Montreal protocol on substances that deplete the ozone layer, Nairobi
5. Eurochlor. Industry Review 2004–2005, to be found under http://www.eurochlor.org/index.asp?page=605 (2007)
6. Schmidhammer L (1988) US Patent 4,754,088
7. Erb J (1993) Environ Prog 12:243
8. Bae JW, Kim IG, Lee JS, Lee KH, Jang EJ (2003) Appl Catal A 240:129
9. Bonarowska M, Malinowski A, Juszczyk W, Karpinski Z (2001) Appl Catal B 30:187
10. Hashimoto Y, Uemichi Y, Ayame A (2005) Appl Catal A 287:89
11. Legawiec-Jarzyna M, Srebowata A, Karpinski Z (2003) React Kinet Catal Lett 79:157
12. Srinivas ST, Jhansi Lakshmi L, Lingaiah N, Sai Prasad PS, Rao PK (1996) Appl Catal A 135:201
13. Yuan G, Lopez JL, Louis C, Delannoy L, Keane MA (2005) Catal Commun 6:555
14. Decker S, Lagadic I, Klabunde KJ, Moscovici J, Michalowicz A (1998) Chem Mater 10:674
15. Ma X, Zheng M, Liu W, Qian Y, Zhao X, Zhang B (2005) Chemosphere 60:796
16. Chien YC, Wang HP, Yang YW (2001) Environ Sci Technol 35:3259
17. Danielsen KM, Gland JL, Hayes KF (2005) Environ Sci Technol 39:756
18. Erbs M, Hansen HCB (1999) Environ Sci Technol 30:307
19. Ma X, Zheng M, Liu W, Qian Y, Zhang B, Liu W (2005) J Hazard Mater 127:156
20. Liu GH, Wang JL, Zhu YF, Zhang XR (2004) Phys Chem Chem Phys 6:985
21. Tamai T, Inazu K, Aika K (2003) Chem Lett 32:436
22. Koper O, Lagadic I, Klabunde KJ (1997) Chem Mater 9:838
23. Koper O, Li YX, Klabunde KJ (1993) Chem Mater 5:500
24. Klabunde KJ, Stark J, Koper O, Mohs C, Park DG, Decker S, Jiang Y, Lagadic I, Zhang D (1996) J Phys Chem B 100:12142
25. Koper O, Wovchko EA, Glass JA, Yates JJT, Klabunde KJ (1995) Langmuir 11:2054
26. Manoilova OV, Podkolzin SG, Tope B, Lercher JA, Stangland EE, Goupil JM, Weckhuysen BM (2004) J Phys Chem B 108:15770
27. Podkolzin SG, Manoilova OV, Weckhuysen BM (2004) J Phys Chem B 109:11634
28. Tamai T, Inazu K, Aika K (2004) Bull Chem Soc Jpn 77:1239
29. van der Avert P, Weckhuysen BM (2002) Angew Chem Int Ed 41:4730
30. van der Avert P, Podkolzin SG, Manoilova OV, de Winne H (2004) Chem Eur J 10:1637
31. van der Avert P, Weckhuysen BM (2004) Phys Chem Chem Phys 6:5256
32. Weckhuysen BM, Rosynek MP, Lunsford JH (1999) Phys Chem Chem Phys 1:3157
33. van der Heijden AWAM, Bellière V, Espinosa Alonso L, Daturi M, Manoilova OV, Weckhuysen BM (2005) J Phys Chem B 109:23993
34. van der Heijden AWAM, Garcia Ramos M, Weckhuysen BM (2007) Chem Eur J 13:9561
35. Milchert E, Pazdzioch W, Myszkowski J (1995) Ind Eng Chem Res 34:2138
36. Carmello D, Finocchio E, Marsella A, Cremaschi B, Leofanti G, Padovan M, Busca G (2000) J Catal 191:354
37. Mile B, Ryan TA, Tribbeck TD, Zammitt MA, Hughes GA (1994) Top Catal 1:153
38. Bozzelli J, Chen Y (1992) Chem Eng Comm 115:1
39. Anderson JR, McConkey BH (1968) J Catal 11:54
40. Frankel KA, Jang BW-L, Roberts GW, Spivey JJ (2001) Appl Catal, A 209:401
41. Mochida I, Uchino A, Fujitsu H, Takeshita K (1976) J Catal 43:264
42. Pouchet CJ (1989) Aldrich library of FT-IR spectra: vapor phase. vol 3. Aldrich Chemical Company, Milwaukee